The current issue and full text archive of this journal is available on Emerald Insight at:
www.emeraldinsight.com/1757-9864.htm

Seismic resistance prediction of corroded S400 (BSt420) reinforcing bars

Charis Apostolopoulos, George Konstantopoulos and Konstantinos Koulouris
Department of Mechanical Engineering and Aeronautics, University of Patras, Patras, Greece

Received 10 February 2017
Revised 21 April 2017
Accepted 24 April 2017

Abstract

Purpose – Structures in seismic areas, during their service lifetime, are subjected to numerous seismic loads that certainly affect their structural integrity. The degradation of these structures, to a great extent, depends on the scale of seismic events, the steel mechanical performance on reversal loads and its resistance to corrosion phenomena. The paper aims to discuss these issues.

Design/methodology/approach – Based on the experimental results of seismic steel behavior S400 (BSt III), which was widely used in the past years, a prediction study of seismic steel behavior was conducted in the current study. This prediction on behavior of both reference and corroded steel was succeeded through a simulation of experimental low cycle fatigue conditions (LCF – strain controlled).

Findings – At the same time, the present study analyses fatigue factors (ef, a, f_{SR}, ed, ep, R, b) that define their inelastic relation between tension – strain and a prediction model on behavior of both reference and corroded steel rebar, in seismic loads conditions (LCF), is proposed.

Originality/value – Moreover, this study dealt with the synergy of corrosion factor and the existence of superficial ribs (ribbed and smoothed) in seismic behavior of steel bar S400 (BSt420). The S-N curves that are exported can be resulted in a first attempt of prediction of anti-seismic behavior on reinforced concrete structures with this the same steel class.

Keywords Buckling, Corrosion damage, Hysteresis loops, Low cycle fatigue, S400 (BSt420) reinforcing steel, Stress-strain predictive model

Paper type Research paper

1. Introduction

The vast majority of structures around the world have a load-bearing structure made of reinforced concrete. The reinforcing steel bars in concrete contribute to the high mechanical performance of the structure providing them with high strength and ductility and also the ability to absorb seismic energy. However, the presence of structures in aggressive environments areas impairs the mechanical performance and their service lifetime. The corrosion effect in the durability of structures renders urgent the need of frequent maintenance or other practices and strategies to control the corrosion phenomenon and its sequences. Over the years, the operation of many reinforced concrete structures has often been disrupted in whole or in part, in order for some appropriate interventions to be conducted for their maintenance (Koch *et al.*, 2002). Cost of corrosion studies have been undertaken by several countries. For instance, results of a study conducted by NACE (Koch *et al.*, 2002) show that the total annual estimated direct cost of corrosion in the USA is a staggering $276 billion, approximately 3.1 percent of the nation's GDP. From the aforementioned facts, it seems logical that corrosion leads to enormous social and economic damage in a society. According to what was mentioned above, over the last decades, many researchers have investigated and shown the negative role of corrosion in reinforcing steel bars estimating, at the same time, the corrosion damage of the aging RC members (Ma *et al.*, 2014).

Even though there are a lot of studies indicating the severe effects in the structural integrity of RC structures due to corrosion and seismic loads, the international

International Journal of Structural Integrity
Vol. 9 No. 1, 2018
pp. 119-138
© Emerald Publishing Limited
1757-9864
DOI 10.1108/IJSI-02-2017-0008

regulations and standards, as Eurocode 2 which is used all over Europe, do not determine rules on how structural engineers can predict the mechanical degradation of RC members. Only in Portugal (2000) and Spain (2008) the required levels are higher than those imposed by Eurocodes, i.e. the perspective level of Agt (class C) for yielding strength higher than 500 MPa is equivalent to 8.0-9.0 percent and at least 8.0 percent in case of $Rp \geq 400$ MPa. The aim of this study is to indicate some predictive models, which may seem significant qualifications in the structural design for durability of RC structures.

Corrosion is an electrochemical phenomenon where the steel tends to return to its original form (ore) forming iron oxides on the surface (rust). Eventually, due to the increase in the volume of the rust (caused by saltwater, due to carbonation, rain) large tensile stresses are developed in the surrounding concrete area resulting in the ejection of the concrete and, ultimately, loss of bond between concrete and reinforcing rebars.

In reinforced concrete structures, the corrosion of steel appears, mainly, in two different aspects: pitting corrosion and uniform corrosion. In the case of pitting corrosion, a locally located material loss takes place on the surface of steel bars creating pits of different depths and geometry that leads to an increase in stress concentration. This could facilitate a rapid increase of microcracks and could even be fatal for the integrity and also working life of the structure.

On the other hand, uniform corrosion causes uniform loss of cross-sectional area of reinforcing bars and at the same time increases the effective stresses developed on the reinforcement. At this point, it is important to underline the great effect of pits on the mechanical behavior of the reinforcing bars as has been observed that the maximum depth of a pit may be 8-10 times more profound than the average depth of the uniform type of corrosion (Wanga *et al.*, 2013). In the study (Apostolopoulos and Kappatos, 2013), the influence of corrosion on the reinforcing steel bars was investigated and showed that there is a significant loss of mechanical properties of rebars over time.

The concrete environment initially protects the steel reinforcement acting as a physical barrier at the contact with the environment because of the high alkalinity of concrete (pH~12.5), which creates a protective thin film at the surface of the steel bar. Through the pores of concrete, aggressive corrosive factors enter in the interior of concrete and since they reach a critical concentration ratio (and the consequent reduction of $pH < 9$), the electrochemical processes of corrosion start.

Besides the continuous exposure of RC structures in a corrosive environment, earthquakes are another factor that limits the serviceability which, to date, is the main criterion for the design of a structure. During an earthquake, the whole structure is subjected to cyclic loading with large deformation amplitudes developing large internal forces in the members of the structure. In the past, Sheng and Gong (1997) demonstrated that seismic loading phenomena can be simulated in the laboratory by low cycle fatigue tests.

Several researchers, like Mander *et al.* (1994) and Kunnath *et al.* (2009), have investigated the deterioration of serviceability of reinforcing steel bars due to low-cycle fatigue (LCF) (earthquake) conditions. The steel bars subjected to cyclic load (load history) exhibit different stress-strain behavior according to monotonic load. Hence, the strain history has a significant effect on the strength loss and ductility loss of rebars. Moreover, inelastic buckling of the reinforcing steel bars has been observed due to compressive applied loads. Kashani *et al.* (2015) and Apostolopoulos and Pasialis (2009) have investigated the impact of inelastic buckling in LCF life or rebars. The main parameters which have an effect on buckling phenomenon are the strain history and slenderness ratio L/D. There is insufficient literature concerning corrosion and LCF interaction. Therefore this study is an attempt to predict the mechanical behavior of corroded steel specimens under low cycle fatigue loading.

In Greece, from the early 1960s to late 1990s, S400 grade steel bars were widely used as reinforcement in RC structures, according to Hellenic code ELOT 959 (1987). This grade of steel is equivalent to BSt420 grade according to DIN 488 standard. Although S400 steel has officially been withdrawn from production since the late 1990s, it still acts as the backbone of reinforced structures aging from 20 to 50 years.

Although the behavior of the concrete has been widely studied in the structural integrity of constructions under high strain rates, the behavior of steel reinforcement in seismic loads has not been completely evaluated.

Due to this lack of data, on steel reinforcement, an analytical prediction of steel behavior was conducted under high strain rates, in low cycle fatigue. For this purpose, the prediction of inelastic stress-strain behavior of corroded reinforcing steel bars in LCF loading was made, based on experimental results that were conducted by Apostolopoulos and Pasialis (2009); Apostolopoulos and Papadopoulos on ribbed and smoothed S400 steel bars.

The material properties and the load patterns (LCF in ±1 percent, ±2.5 percent, ±4 percent) have been assumed in agreement with Apostolopoulos and Pasialis (2009), in order to have a calibration and validation of the response of prediction models.

Due to the combined effect of cyclic loading during earthquakes and corrosion phenomena in the long term, the present study is a contribution for the structural engineer to estimate the remaining loading capacity of these structures.

2. Experimental procedure

The experiments were conducted on S400 grade of steel reinforcing bars, specially produced for the needs of the current investigation by a Greek steel mill. The chemical composition of steel S400 is shown in Table I. The material was delivered in the form of 10 mm nominal diameter of ribbed bars according to the studies by Apostolopoulos and Pasialis (2009) and Apostolopoulos and Papadopoulos.

2.1 Salt spray corrosion

The specimens were pre-corroded through accelerated laboratory corrosion tests in salt spray environment. Salt spray tests were conducted according to the ASTM standard B117 (1997) specification. For the tests, a special apparatus, model SF 450 specially designed by C and W. Specialist Equipment Ltd was used. The salt solution was prepared by dissolving five parts by mass of sodium chloride (NaCl) into 95 parts of distilled water. The duration times of exposure were 10, 20, 30, 45, 60 and 90 days. Upon completion, the specimens were washed with clean running water to remove the remaining salt deposits from their surfaces and then were dried. The oxide layer was removed using a bristle brush, according to the ASTM standard G1-03 (2011) specification. Following the cleaning process, the mass loss rate of specimens was determined.

2.2 Tensile tests

In order to make a more comprehensive study of the mechanical behavior of the steel, except LCF tests, additional tensile tests on ribbed bars were performed before and after corrosion, Tensile results are shown in Table II and Figure 1.

Table I. Chemical composition of S400 (wt. %)

C	Mn	S	P	Si	Ni	Cr	Cu	V	Mo	N
0.35	0.94	0.026	0.013	0.26	0.10	0.16	0.42	0.002	0.023	0.010

2.3 LCF tests

The experimental results stem from the research works by Apostolopoulos and Pasialis (2009). More specific, specimens with 170 mm total length and 60 mm in gauge length were cut for the LCF test. The gauge length was equal to six times the nominal diameter of steel specimens.

In advance of the tests, the specimens were divided into two groups in order to investigate the effect of ribs in LCF. The first group was intended directly for LCF tests. The second was submitted to a special treatment in which ribs were totally removed by means of filing from the central gauge area of the specimens.

3. Principles of prediction

3.1 Fatigue life prediction

The LCF life of reinforcing bars has been studied by several researchers though the effe ct of corrosion is often omitted. The current study examines the fatigue life prediction of material based on Coffin-Manson's and Koh-Stephen's models, which are the most popular among the researchers. The Coffin-Manson model relates the plastic strain amplitude (ε_p) to fatigue life:

$$\varepsilon_p = \varepsilon'_f (2N_f)^c \tag{1}$$

	0 days	30 days	90 days
Yield strength (MPa)	454.86	452.53	437.61
Tensile strength (MPa)	695.12	695.29	674.93
Strain Ag (%)	15.53	12.88	9.00
Total strain Agt (%)	19.73	15.33	10.53
Energy density (MPa)	126.56	97.98	63.98

Table II.
Tensile test results

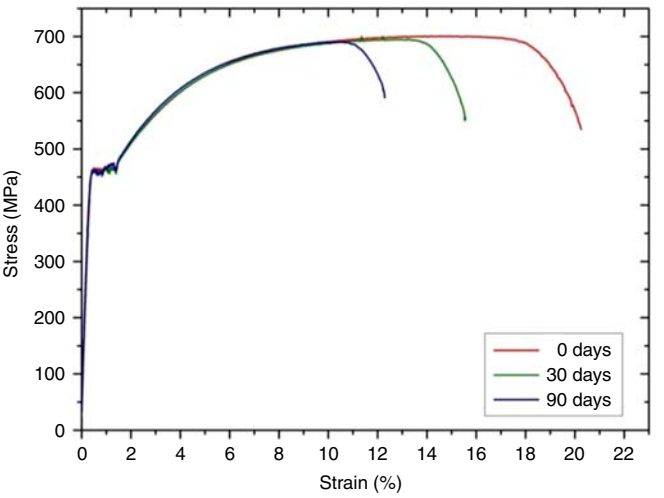

Figure 1.
Stress – strain diagrams of non-corroded and corroded ribbed bars

where ε'_f is the ductility coefficient, i.e. the plastic fracture strain for a single load reversal, c is the ductility exponent and $2N_f$ is the number of half-cycles (load reversals) to failure.

Koh-Stephen extended the Coffin-Manson's model for modeling the LCF life of materials based on the total strain amplitude (elastic strain+plastic strain) as described by the following equation:

$$\varepsilon_\alpha = \varepsilon_f (2N_f)^\alpha \tag{2}$$

where ε_f is the ductility coefficient, i.e. the total fracture strain for a single load reversal, α is the ductility exponent and $2N_f$ is the number of half-cycles (load reversals) to failure.

Between these two models, Koh-Stephen's model was used for the analysis and the prediction of LCF life of reinforcing bars. Furthermore, the influence of corrosion on fatigue material constants, ε_f and α, was explored. The Koh-Stephen equation was fitted to the observed experimental data of each exposure time to calibrate the fatigue material constants (ε_f and α).

3.2 Strength loss prediction

In a similar way, using the Coffin-Manson model, the prediction of strength loss of hysteresis loops was conducted. The prediction of strength degradation of reinforcing bars was made by using a type expression:

$$\varepsilon_{\text{pl}} = \varepsilon_d (f_{\text{SR}})^\alpha \tag{3}$$

Where, ε_d and α are material constants and f_{SR} is the strength loss factor per cycle as measured in a fatigue test at a constant plastic strain amplitude of ε_{pl}. The results of fatigue life and strength loss material coefficients are shown in Tables III and IV.

3.3 Modeling of LCF behavior

The adopted method to analyze the non-linear behavior of steel rebar submitted to cyclic loads constitutes an aspect of the well-known Guiffre-Menegotto-Pinto model, that was initially proposed by Guiffre and Pinto (Giuffre and Pinto, 1970) and implemented later by Menegotto and Pinto (Menegotto and Pinto, 1973). The initial form of this model does not take into consideration the Bauschinger effect. In this model, the cyclic behavior via a stress-strain relation of steel rebars is represented. The envelope curve related to loading, unloading and reloading is described by the following equation form:

$$f' = b\varepsilon' + \frac{(1-b)\varepsilon'}{\left(1+\varepsilon'^R\right)^{1/R}} \tag{4}$$

Days of corrosion	Mass loss (%)	Smoothed bars			Ribbed bars		
		ε_f	α	R^2	ε_f	α	R^2
0	0	0.1036	−0.296	0.994	0.1040	-0.314	0.986
10	1.58	0.1107	−0.33	0.989	0.1110	−0.351	0.952
20	2.50	0.1060	−0.337	0.973	0.1139	−0.367	0.985
30	3.77	0.1063	−0.339	0.985	0.1153	−0.372	0.981
45	5.18	0.929	−0.331	0.987	0.1212	−0.391	0.975
60	7.23	0.1173	−0.388	0.971	0.1032	−0.361	0.998
90	8.48	0.1151	−0.393	0.999	0.1039	−0.363	0.998
Mean*		0.1081	−0.353		0.1114	−0.368	

Note: *Mean value of corroded steel samples

Table III. Fatigue Life material constants

Table IV.
Strength Loss material constants

Days of corrosion	Smoothed bars			Ribbed bars		
	ε_d	α	R^2	ε_d	A	R^2
0	0.0176	0.369	0.934	0.0169	0.411	0.979
10	0.0169	0.421	0.958	0.0162	0.444	0.981
20	0.0146	0.490	0.992	0.0145	0.507	0.978
30	0.0148	0.466	0.974	0.0138	0.516	0.981
45	0.0129	0.531	0.994	0.0135	0.477	0.972
60	0.0123	0.593	0.991	0.0131	0.554	0.973
90	0.0119	0.535	0.986	0.0124	0.521	0.972
Mean*	0.0139	0.506		0.0139	0.503	

Note: *Mean value of corroded steel samples

The accompanying terms consist of a modified form of that proposed by Filippou *et al.* (1983) and are defined as:

$$\varepsilon' = \frac{\varepsilon_s - \varepsilon_Q}{\varepsilon_P - \varepsilon_Q}, \quad f' = \frac{f_s - f_Q}{f_P - f_Q}, \quad b = \frac{E_{\text{sh}}}{E_s} \tag{5}$$

The objective of the above modification, i.e. the insertion of an extra parameter $\varepsilon_Q \varepsilon_Q$, f_Q, was not only to improve the accuracy of the model but also to incorporate an extra point that contributes to the approach of the Bauschinger effect, in the case where buckling phenomenon does not exist.

The above equation represents a curved transition from a straight line asymptote with slope E_s to another asymptote with slope E_{sh}. The position of the latter asymptote corresponds to the yield surface, is assumed to be constantly shifted as well as the slope E_s (Figure 2). More specific, both the E_{sh} slope and the slope of E_s are prone to diminishing.

The parameters f_Q and ε_Q are the stress and strain at the inception point of the envelope curve. It should be noted that the unloading part of hysteresis branch initially takes place along a line parallel to the elastic region. The end of this linear unloading part constitutes

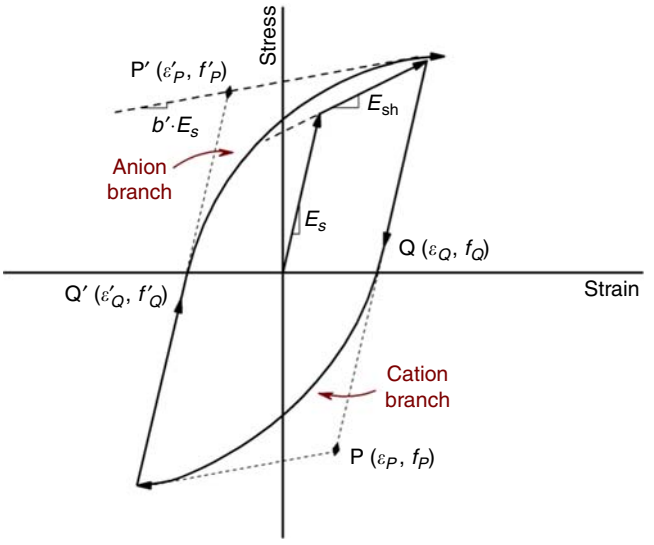

Figure 2.
Representation of model and parameters

the inception point of transition branch that refers to Q point. The parameters f_P and ε_P are the stress and strain at the point where the two asymptotes of the branch, under consideration, meet (point P). From that point, the transition from tension to compression (and vice versa) follows a branch curve that forms a smooth "knee" that is located at the point of theoretical yielding point, in the case of monotonic loading. The term b is the strain hardening ratio defined as the ratio between slope E_{sh} and E_s. R is a parameter that influences the shape of the transition curve.

The main reason for adopting the model of Menegotto and Pinto relies on the fact that each parameter defines a different geometry of the envelope curve and therefore the parameters can be easily determined from the experimental data.

As indicated in Figure 2, the coordinates P (ε_P, f_P) and Q (ε_Q, f_Q) are updated after each strain reversal. Each loading cycle contains two transition branches; the anion branch corresponding to positive, tensile loads and the cation branch corresponding to negative, compression loads. The coordinates P′ and Q′ refer to the anion transition curve.

The determination of the coordinates Q and P, as for cation branch, and Q′ and P′, as for anion branch of the envelope curve, was based on experimental data. By isolating the cation and the anion envelope curve from each cycle, in combination with the modified mathematical model, the parameters R, b and R', b' were specified, respectively. For the purpose of simplifying the modeling process, the variance of parameters was basically approached through linear fitting.

4. Results – discussion

The results of mechanical tensile tests of ribbed bars are presented in Table II. Herein, it is shown that the decrease of strength properties is (about) equivalent to mass loss decrease, opposite to the ductility properties where a dramatic decrease is presented. Since it is widely known that corrosion of embedded steel bars initially (for mass loss rates 1.5-2 percent) has a positive impact on bonding between concrete and steel bar, the prediction of seismic loads behavior (low cycle fatigue) will have as reference some experimental results from 1.58 percent to higher percentage level of mass loss. However, the analysis of experimental results of low cycle fatigue tests, through the statistical regression analyses, shows that there are fatigue life prediction models for 0-8.48 percent mass loss.

The derived predictive curves were based on Table III, where the low cycle fatigue test results are presented. Figures 3 and 4 represent the curves of the prediction model for each level of corrosion experimentally examined along with the predictive curve developed that illustrates the average influence of corrosion impact with regard to 1.58-8.48 percent range of mass loss rate with dashed line.

In Table IV, the calibrated material constants of fatigue life, ε_f and α, are presented in consequence of regression analysis. The results come from material model show high convergence reliability (values of R^2). The analysis of empirical constants (mean) ε_f and α of life prediction model reflects the influence of the corrosive factor on corrosion level of steel rebar. For both types of steel bar (ribbed and smoothed) the prediction model resulted from these mean values. The curves of the two prediction models are in a good agreement with the experimental results taking into account the fatigue phenomena, corrosion damage and buckling effect. As it was expected, corrosion negatively affects the life expectancy of steel specimens.

It is obvious from Figures 3 and 4 that by increasing the exposure time, the life expectancy of material is steadily decreased. From the early exposure times of specimens, in smaller strain amplitude (mainly in ±1 percent, ±2.5 percent), shorter life expectancy is recorded. On the contrary, in larger strain ranges (±4 percent) just as Kashani *et al.* (2015) study, so to the present study, additional negative phenomena are highlighted due to the effect of inelastic buckling that is predominating.

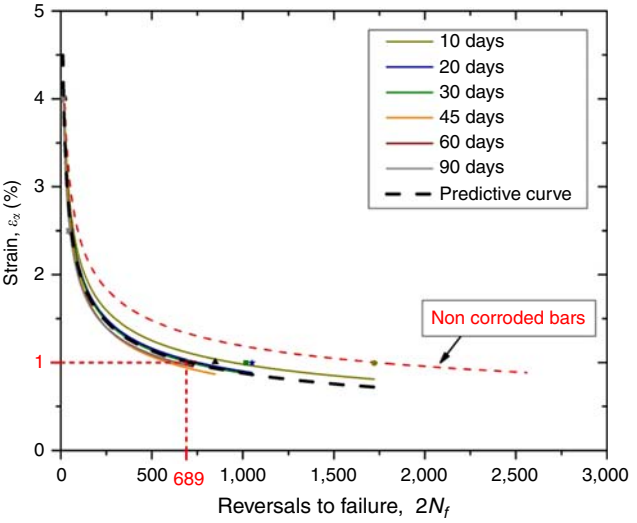

Figure 3.
Fatigue life of corroded ribbed bars

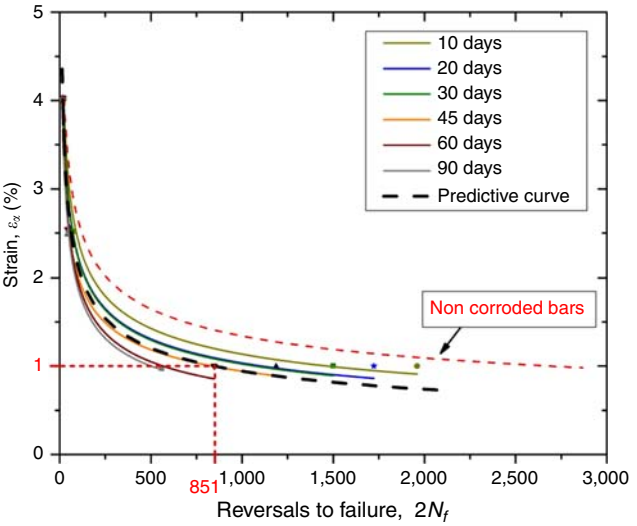

Figure 4.
Fatigue life of corroded smoothed bars

The results from the investigation of the contribution of steel ribs are depicted in Figures 3 and 4. It is observed that for the same number of reversals ($2N_f$), the maximum deformation of specimens without ribs is higher than that of ribbed specimens. In the same manner, for a given range of deformation (e.g. ±1.0 percent) the number of reversals of ribbed bars is presented lower over the respective of smoothed bars.

According to the modified Coffin-Manson's equation that is referred to the coefficient of strength loss per fatigue cycle, in terms of plastic deformation (Kunnath *et al.*, 2009), a prediction model of strength loss as a function of loading cycles was developed.

In this analysis, the coefficient f_{SR} was estimated by calculating the total strength loss to the cycle preceding failure and dividing by the total number of cycles till fracture.

The failure cycle was not considered since it may be accompanied by significant strength degradation due to necking formation.

The results of the experimental procedure led to the prediction modeling of strength loss per loading cycle fatigue of S400 steel with and without ribs i.e. ribbed and smoothed bars, respectively.

In the following diagrams (Figures 5 and 6) the modified Coffin-Manson equation is displayed, fitted to the experimental data using non-linear regression analysis. The results of regression analyses are summarized in Table V.

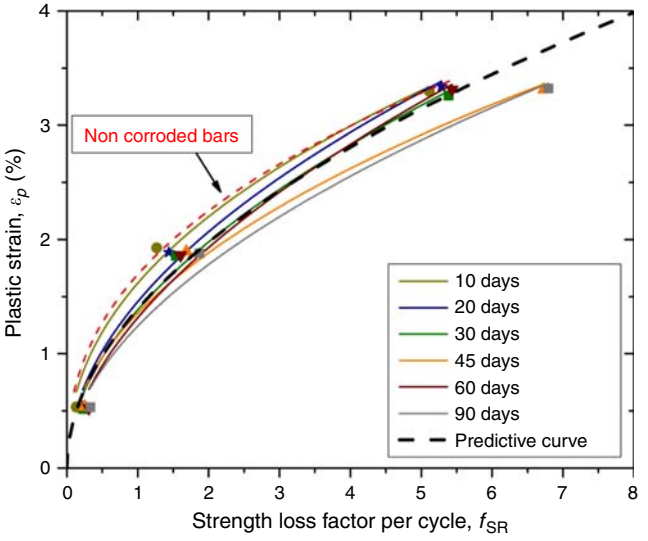

Figure 5.
Strength loss of corroded ribbed bars

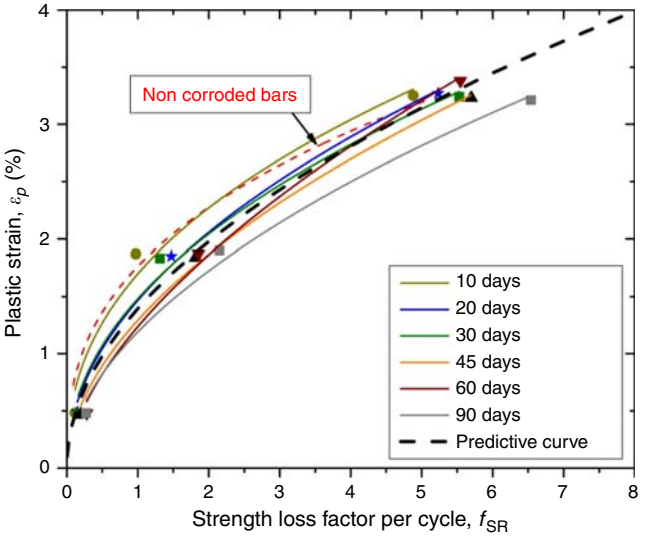

Figure 6.
Strength loss of corroded smoothed bars

In Figures 5 and 6, the strength loss factor per loading cycle as a function of imposed plastic strain rate is illustrated. As can be seen both, in two diagrams, at lower levels of plastic deformation (almost zero) all fitting curves coincide with each other since the steel rebars behave elastically and therefore they can entirely recover their load-bearing capacity over loading cycle.

In addition, a slight divergence is observed between the curves for plastic strain rates near to 1.5-3 percent. In that range of plastic strain, the influence of corrosion damage is considered as significant. In particular, a higher level of corrosion corresponds to the higher level of f_{SR} coefficient. For greater rates of plastic strain the model curves, almost, converge and tend to coincide with each other as a result of buckling phenomena that are generated and dominate on the mechanical performance of steel over the forthcoming corrosion damage.

In order to evaluate the equivalent corrosion damage in the frame of the natural corrosive environment, such as coastal or marine regions, a connection with the artificial corrosion damage of salt spray method is required.

An effort to correlate natural corrosion and accelerated laboratory corrosion of exposed rebars (bare samples) has been made in previous work (Papadopoulos *et al.*, 2011). In that study, an accelerated factor had been estimated taking into account the corrosion attack rate (mm/year) and the mass loss rate for each case, respectively. Concerning mass loss rate, the value of the accelerated factor was about 79. Hence, in the case of 90 days in salt spray chamber (corresponding to 10 percent mass loss and Ø10 nominal diameter) the equivalent time of exposure in the natural corrosive environment would be about 20 years in an intense coastal environment.

Furthermore, the production process of S400 grade of steel (Hot-Rolled method) and the consequent microstructure form of rebar (single-phase type) allows the results above to be used for the prediction of mechanical behavior referring to steel rebars with cross-section area greater than Ø10.

The assumption above derives from the fact that the depth of corrosion damage over corrosion period is equivalent regardless of steel bars cross-section area, especially when corrosion quality tends to approach the uniform type of corrosion.

In that case, it would be expected that the reinforcement of RC structures dated up to 20 years (and even more) could have been damaged in the same way as steel rebars in this study, in terms of life expectancy and also strength degradation (Fatigue damage) during a loading event such as an earthquake.

Figures 7 and 8 (left), depict the radius R and R' of the curve of transition branch. Based on the study of the parametric equation of the model and the results of regression analysis, it was noticed that the variance of the values is limited, it does not significantly affect the

Table V.
Cycles before load capacity drops below 80 percent of the maximum value for ±4 percent strain level

Days of salt spray corrosion	0	45	60	90
Number of cycles				
Tensile loads	10	8	6	5
	9	8	6	3
	9	10	5	3
			5	2
Mean	9	8	5	3
Compressive loads	5	4	2	0
	5	4	2	0
	5	5	2	0
			2	0
Mean	5	4	2	0

prediction and therefore the parameter R and R' were represented by horizontal lines of average value R_{av} and R'_{av}, respectively.

Figures 7 and 8 (right) depict the variation of parameter b as a function of number of loading cycles. From the investigation of the transition branch function, it was observed that b parameter significantly influences the envelope curve and the maximum load value (strength degradation), both the parameters b referring to cation branch and the parameters b' referring to anion transition branch. It is obvious that both parameters b and b' have a rising course over fatigue cycles, so the strength degradation per cycle was accompanied by an increase of parameters b and b'. For the development of prediction model, in accordance with LCF experiment, it was adopted a linear fit based on the regression analysis results, in the case of corroded and non-corroded steel bars.

In Figures 9 and 10, the distribution of the coordinates of point Q and Q′ is depicted defined as the point of the section of the linear branch of the material and the inception part of transition branches. According to the fact that the ability of material for elastic deformation is reduced in the long run, the coordinates of Q point show an algebraic decreased behavior and the respective of Q′ point an increased behavior. The approach of the coordinates Q and Q′ was based on linear type functions. It should be noted that the variation of ε_Q (and also ε'_Q) is almost negligible as the range of the parameter is limited enough. However, the values of f_Q (and also f'_Q) significantly affect the predictive model since they indicate the beginning of the transition branch.

In Figures 11 and 12, it is depicted that the variation of the coordinates of point P and P′ define the theoretical yielding points. The position of P and P′ is directly influenced by the strength degradation per loading cycle. As a result, the coordinates of P shows an increased behavior while the coordinates of P′ shows a decreased behavior. For the needs of

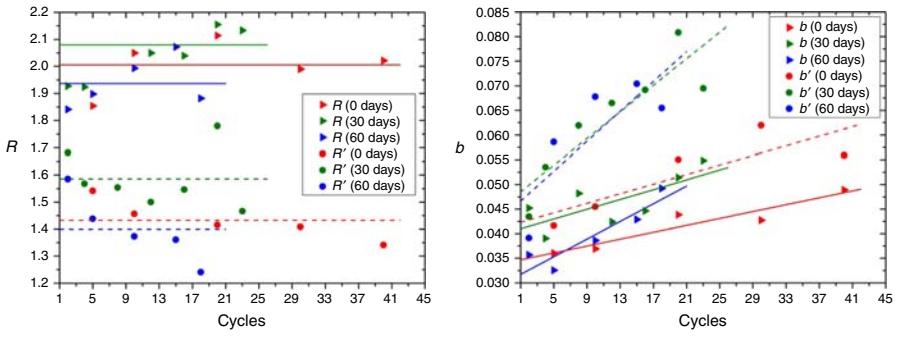

Figure 7. Parameter R-R' (left) and b-b' (right) as a function of number of cycles for corroded and non-corroded rebars (±2.5 percent imposed deformation)

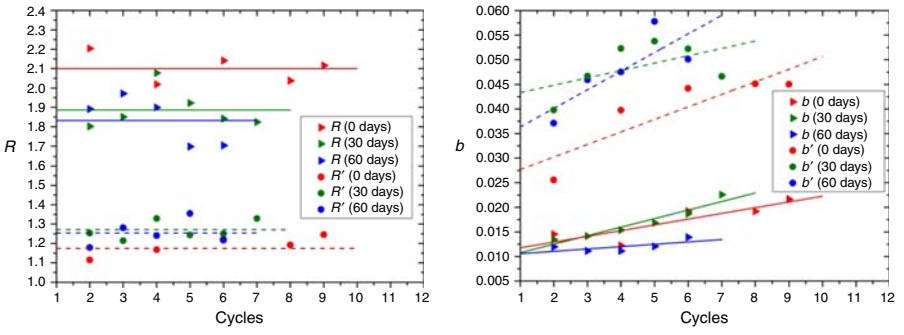

Figure 8. Parameter R-R' (left) and b-b' (right) as a function of number of cycles for corroded and non-corroded rebars (±4.0 percent imposed deformation)

prediction, the adjustment of the coordinates was made through linear type function. Herein, it is observed that the linear functions refer to ±4 percent imposed deformation of corroded steel does not show any significant difference in comparison with that of non-corroded rebar due to the dominant buckling phenomena, in that case. On the contrary, in the case of ±2.5 percent deformation level it is observed a slight reduction in the strain and stress values between the corroded and non-corroded rebar in the case of cation branch in the same way as for anion branch, although this effect is negligible in some cases. It can be seen from Figures 11 and 12 (right), as corrosion damage proceeds the slope of the parameter f_Q (or f'_Q) adjusted line increases, in the case of ±2.5 percent. On the other hand, in the case of ±4 percent, the corresponding difference in slope is very small because of the existing buckling phenomena.

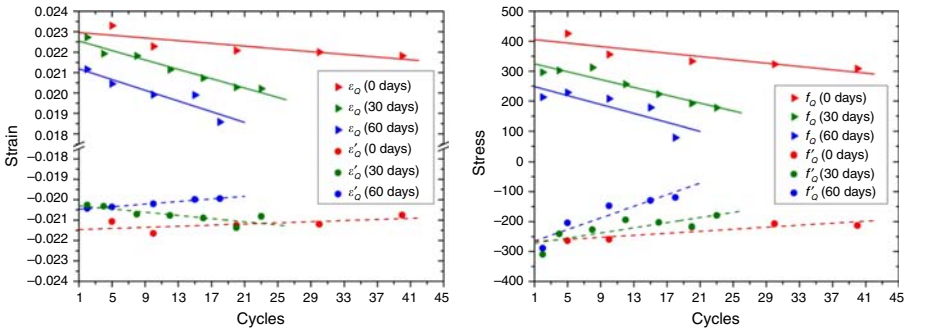

Figure 9.
Parameter of strain (point Q) and stress (point Q) as a function of number of cycles for corroded and non-corroded rebars (±2.5 percent imposed deformation)

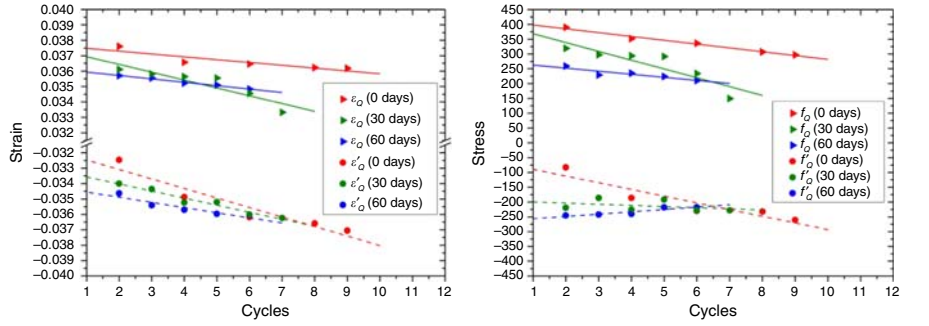

Figure 10.
Parameter of strain (point Q) and stress (point Q) as a function of number of cycles for corroded and non-corroded rebars (±4.0 percent imposed deformation)

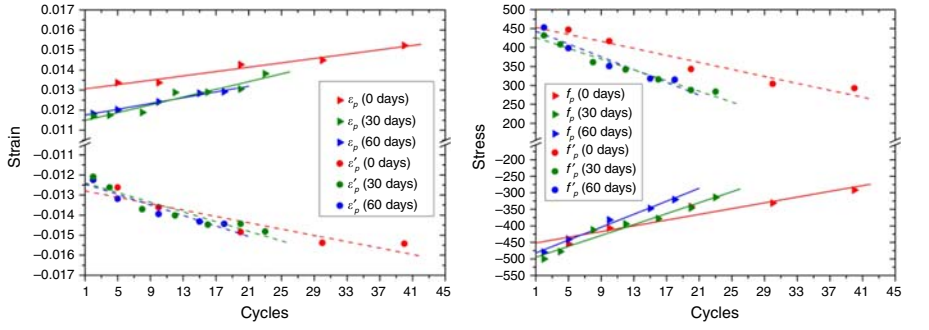

Figure 11.
Parameter of strain (point P) and stress (point P) as a function of number of cycles for corroded and non-corroded rebars (±2.5 percent imposed deformation)

Relied on the adjusted curves from the graphs above, the predicted behavior of steel bar (of the hysteretic branch) was conducted through a code in a MatLab programming language. In this code, the adjusted functions of defined parameters in concert with the calibrated experimental data of fatigue life prediction, for a certain strain level (Figure 13), were inserted in the code in case of non-corroded and corroded for 30 and 60 days, respectively.

The connection of cation and anion transition branches, in each cycle of the model, was accomplished in order to depict the stress-strain dependence of hysteretic branches according to LCF diagram. A comparison between the experimental results and the aforementioned prediction material model follows, based on the parameters developed

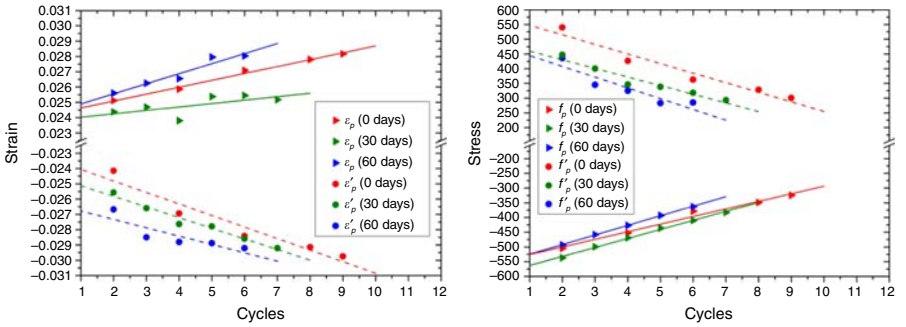

Figure 12.
Parameter of strain (point P) and stress (point P) as a function of number of cycles for corroded and non-corroded rebars (±4.0 percent imposed deformation)

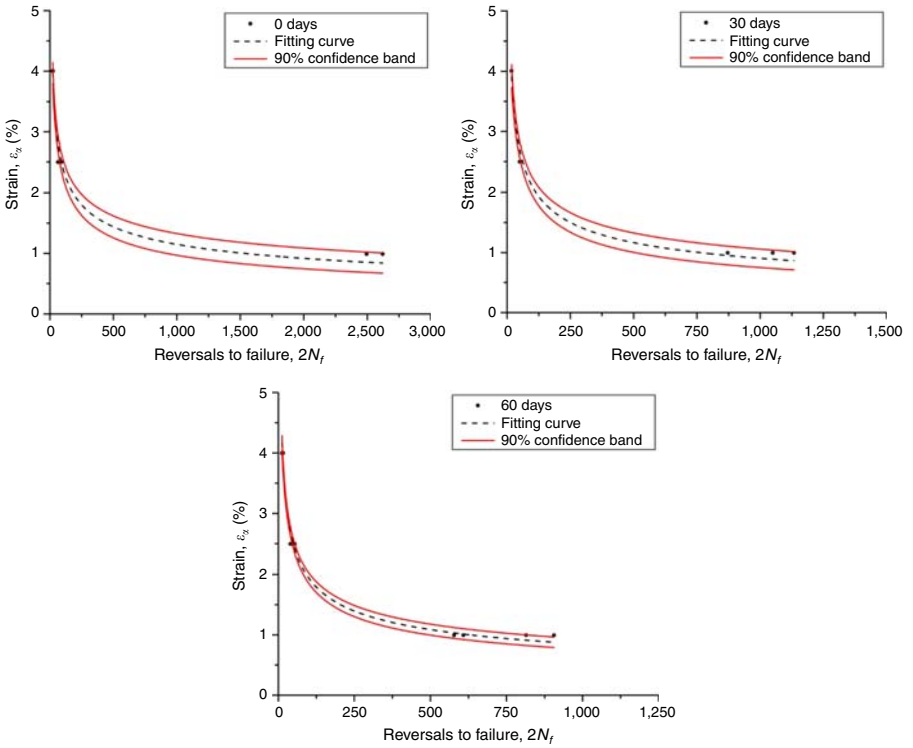

Figure 13.
Calibrated experimental data of fatigue life prediction for non-corroded and corroded steel rebars

in this study. Figures 14-16 (left and right) depict the comparison of the experiment and the model for two different imposed deformation rates (±2.5 percent and ±4 percent) of non-corroded and corroded for 30 and 60 days steel rebars.

From Figures 14-16, it is observed that the prediction model is in a good agreement with the experimental results. The variation of the maximum loads level (section A and B), under the progress of cyclic loads, is in the range of 10-15 MPa at the most. This variation is acceptable as the experimental results of steel bar differ from test to test. Furthermore, remarkable is the fact that the prediction model is able to simulate the buckling phenomenon in a sufficient manner being in a good agreement with the experimental results, including an internal error up to 10 percent.

In order to investigate further the impact of corrosion and loading event on mechanical performance of rebars in reinforced concrete structures, a complementary study by means of load bearing ability of steel bars was established.

Figure 17 depicts the gradual reduction of maximum receiving load per loading cycle in the case of ±4 percent imposed strain rate. Herein, it is initially observed a rapid increase of the exerted force that takes place during the first cycle, due to hardening of the material. Following that, a gradual reduction of the exerted force is observed for most of the specimens' life followed by a new rapid drop that continues until the failure of the specimen.

The steel reinforcement used in RC structures, however, is expected to carry a constant load throughout its service life, since the exerted loads on load carrying elements of such structures remain fairly constant over time.

Furthermore, an overall reduction of the exerted force is observed as the corrosion level increases, as for tensile loads in the same way as for compressive loads. By defining a lower limit of 80 percent of the maximum load of non-corroded steel bar, it can be seen that the beneficial number of cycles is dramatically reduced. The ongoing reduction of load bearing ability further to that threshold is considered as a strong reason for the deconstruction of concrete in RC members.

In addition, under the influence of corrosion damage even though the useful number of cycles is getting limited, concerning tensile loads, it is observed that in the case of compressive loads the equivalent threshold, in some cases, is not met. A possible explanation for that could be the intense buckling phenomena that are generated under high strain levels.

The total number of cycles for which the set threshold is met is given in Table V. Table VI presents the overall low cycle fatigue test results in different amplitudes of deformation ±1 percent, ±2.5 percent, and ±4 percent for four cases of corrosion level. The acceptable limits of maximum tensile and compression receiving load are depicted in Figure 17.

In that case, the existing buckling phenomena and the level of corrosion induce a prompt and also significant reduction of load-bearing capacity and consequently endurance of material.

5. Conclusions

In this study, the effect of corrosion on the mechanical performance of S400 grade of steel bar was investigated. More specific, the degradation of maximum strength and the life expectancy were examined based on fatigue life and strength loss prediction models, due to LCF and corrosion effect. Furthermore, a simplified hysteretic model was conducted so as to simulate the non-linear dynamic response of reinforcing bars representing at the same time the effect of inelastic buckling and LCF strength degradation as well. At this point, a complementary study of predicting the performance and the useful service life of a reinforced concrete member was demonstrated by introducing an upper tensile as well as compressive load threshold of the steel reinforcing bar.

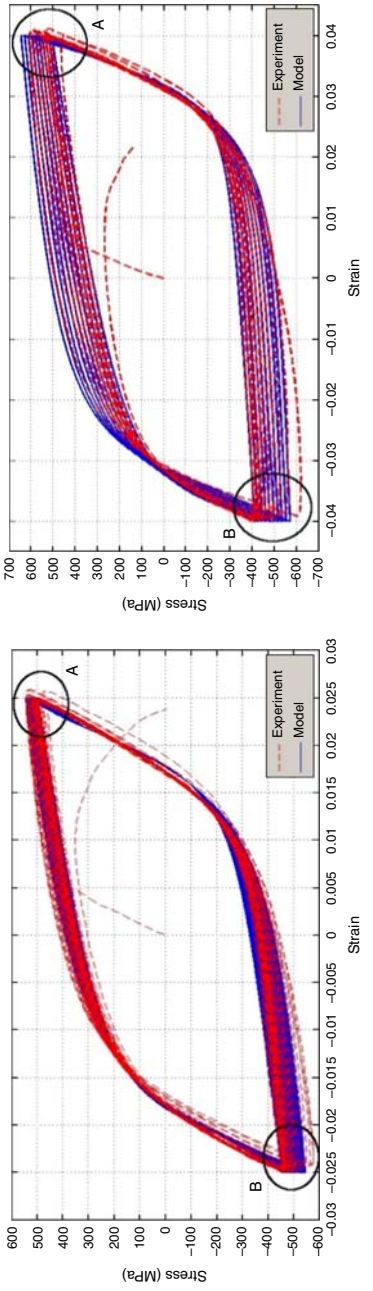

Figure 14.
Comparison of the experimental results and the proposed analytical model of non-corroded rebar at ±2.5 percent (left) and ±4.0 percent strain amplitude (right)

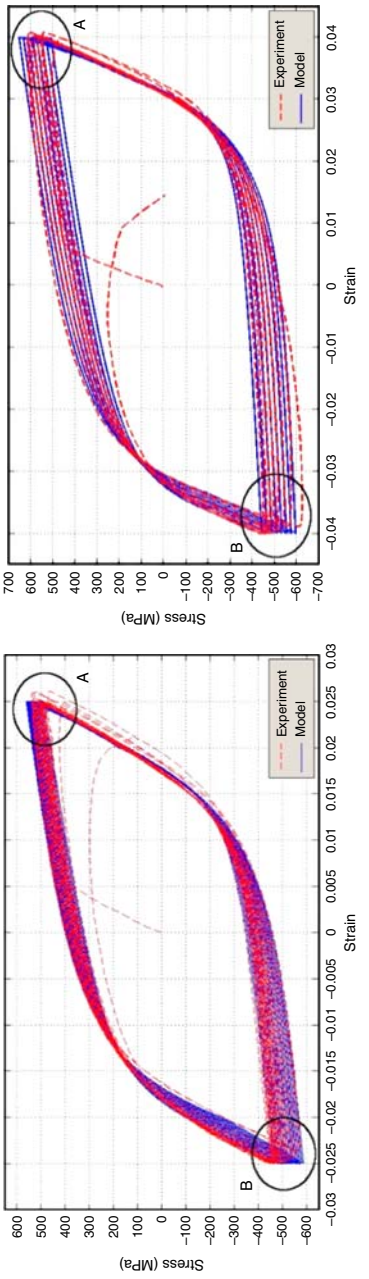

Figure 15.
Comparison of the experimental results and the proposed analytical model of corroded for 30 days rebar at ±2.5 percent (left) and ±4.0 percent strain amplitude (right)

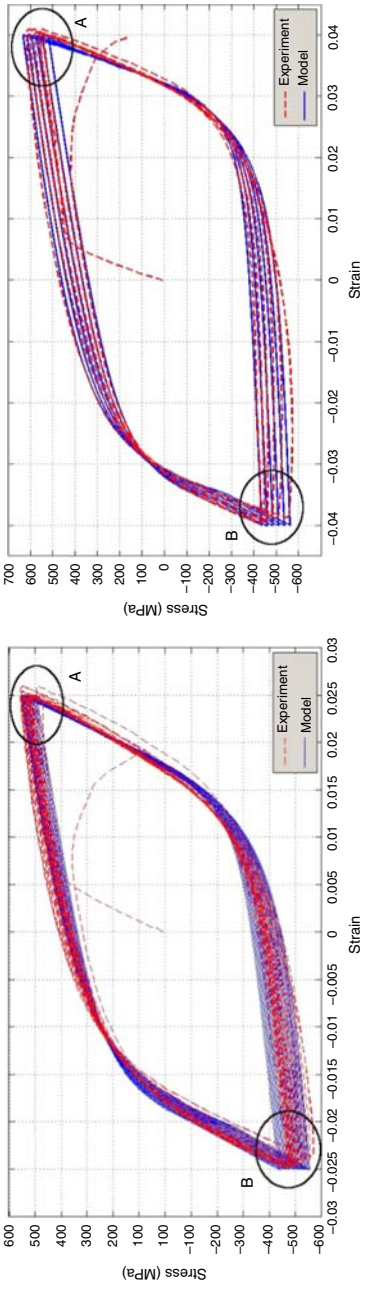

Figure 16.
Comparison of the experimental results and the proposed analytical model of corroded for 60 days rebar at ±2.5 percent (left) and ±4.0 percent strain amplitude (right)

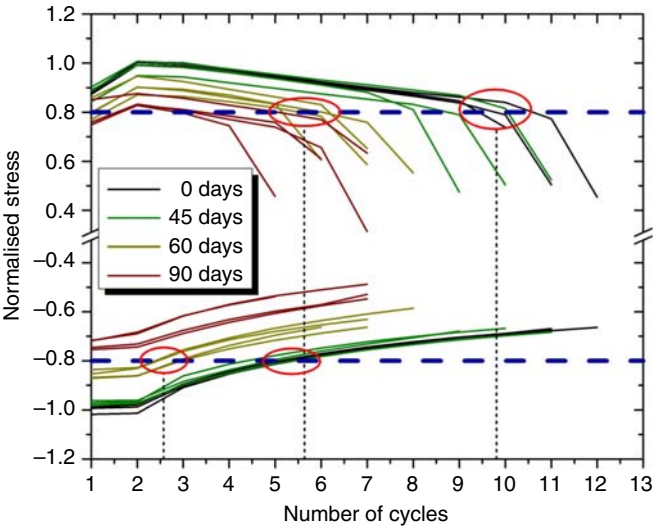

Figure 17.
Cycles before load capacity drops below 80 percent of the maximum tensile and compressive value for ±4 percent strain level

		Ribbed bars		Smoothed bars	
Days of corrosion	Strain amplitude (%)	Cycles to fracture	Dissipated energy (MPa)	Cycles to fracture	Dissipated energy (MPa)
0	±1.0	1,280	7,103	1,435	7,420
	±2.5	40	1,059	51	1,334
	±4.0	11	537	12	579
45	±1.0	424	2504	594	3,281
	±2.5	24	629	26	681
	±4.0	10	470	8	353
60	±1.0	363	2,151	424	2,214
	±2.5	24	627	24	605
	±4.0	7	337	8	359
90	±1.0	349	1,862	365	2040
	±2.5	24	587	24	626
	±4.0	7	272	7	344

Table VI.
Low cycle fatigue test results

Source: Apostolopoulos and Pasialis (2009)

The main outcomes of this study can be summarized as follows:

- The corrosion level, as a parameter, has a negative effect on the seismic performance of steel rebar.
- The non-corroded bars show a ductile failure mechanism compare to corroded bars. This is also observed in the case of smoothed compared to ribbed bars. However, as the strain amplitude increases the influence of ribs are reduced and the fracture of bars is mainly governed by the stress concentration of buckling phenomena.
- In the case of ±4 percent imposed deformation, the corrosion impact has a minor effect on the cycle's life of rebar. The LCF performance is mainly governed by the buckling effect.
- The results of predicting material model can also be used for the evaluation of the entire existed S400 steel rebars in RC structures, with greater cross-section areas, as they constitute a single phase steel material.

- The simplified fitting curves of defined parameters are able to simulate the experimental data and, at the same time, to sufficiently predict the experimental results including the inelastic buckling and corrosion effect.
- The force – fatigue cycles analysis indicate that the designer engineer should take into consideration a part of cycles number and not the total cycles to failure of rebar. A drop of the initial strength (up to 80 percent) could destroy the concrete – steel cohesion.

References

Apostolopoulos, C. and Kappatos, V. (2013), "Tensile properties of corroded embedded steel bars B500c in concrete", *International Journal of Structural Integrity*, Vol. 4 No. 2, pp. 275-294.

Apostolopoulos, C. and Pasialis, V.P. (2009), "Effects of corrosion and ribs on low cycle fatigue behavior of reinforcing steel bars S400", *Journal of Materials Engineering and Performance*, Vol. 19 No. 3, pp. 385-394.

ASTM Standard B117 (1997), *Standard Practice for Operating Slat Spray (Fog) Apparatus*, ASTM Intern., West Conshohocken, PA, doi: 10.1520/B0117-97.

ASTM Standard G1-03 (2011), *Standard Practice for Preparing, Cleaning, and Evaluating Corrosion Test Specimens*, ASTM International, West Conshohocken, PA, doi: 10.1520/G0001-03R11.

ELOT 959 (1987), *Hellenic Standard for the Steel Reinforcement of Concrete*, Greek organization of standardization, Athens.

Filippou, F.C., Popov, E. and Bertero, V. (1983), "Effects of bond deterioration on hysteretic behavior of reinforced concrete joints", Report EERC 83-19: Earthquake Engineering Research Center, University of California, Berkeley, p. 184.

Giuffre, A. and Pinto, P. (1970), "2nd comportamento del cemento armato per sollecitazioni cicliche di forte intensita", *Giornale del Genio Civile*, Vol. 1 No. 5, pp. 391-408.

Kashani, M.M., Barmi, A.K. and Malinova, V.S. (2015), "Influence of inelastic buckling on low-cycle fatigue degradation of reinforcing bars", *Construction and Building Materials*, Vol. 94, pp. 644-655.

Koch, G.H., Brongers, M.P.H., Thompson, N.G., Virmani, Y.P. and Payer, J.H. (2002), "Corrosion costs and preventive strategies in the United States", Publication No. FHWA-RD-01-156, Federal Highway Administration, McLean, VA.

Kunnath, S.K., Heo, Y.A. and Mohle, J.F. (2009), "Nonlinear uniaxial material model for reinforcing steel bars", *Journal of Structural Engineering*, Vol. 135 No. 4, pp. 335-343.

Kunnath, S.K., Kanvinde, A., Xiao, Y. and Zhang, G. (2009), "Effects of buckling and low cycle fatigue on seismic performance of reinforcing bars and mechanical couplers for critical structural members", Technical Report CA/UCD-SESM-09-01, California Department of Transportation, Sacramento, CA.

Ma, Y., Y, Xiang, L, Wang, J, Zhang and Y, Liu (2014), "Fatigue life prediction for aging RC beams considering corrosive environments", *Engineering Structures*, Vol. 79, pp. 211-221.

Mander, J.B., Panthaki, F.D. and Kasalanati, A. (1994), "Low cycle fatigue behavior of reinforcing steel", *Journal of Materials in Civil Engineering*, Vol. 6 No. 4, pp. 453-468, doi: 10.1061/(ASCE) 0899-1561(1994)6:4(453).

Menegotto, M. and Pinto, P.E. (1973), "Method of anaysis for cyclically loaded reinforced concrete plane frames including changes in geometry and non-elastic behavior of elements under combined normal force and bending", *IABSE Symposium of Resistance and Ultimate Deformability of Structures Acted on by Well-Defined Repeated Loads, International Association of Bridge and Structural Engineering, Libson*, Vol. 13, pp. 15-22.

Papadopoulos, M.P., Apostolopoulos, C., Zervaki, A.D. and Haidemenopoulos, G.N. (2011), "Corrosion of exposed rebars, associated mechanical degradation and correlation with accelerated corrosion test", *Construction and Building Materials*, Vol. 25 No. 8, pp. 3367-3374.

Sheng, G.M. and Gong, S.H. (1997), "Investigation of low cycle fatigue behavior of building structural steels under earthquake loading", *Acta Metallurgica Sinica (English Letters)*, Vol. 10 No. 1, pp. 51-55.

Wanga, Xiao-gang, Wei-ping, Zhang, Xiang-lin, Gu and Hong-chao, Dai (2013), "Determination of residual cross-sectional areas of corroded bars in reinforced concrete structures using easy-to-measure variables", *Construction and Building Materials*, Vol. 38, pp. 846-853.

Further reading

DIN 488-3 (1986), *Reinforcing Steel Bars Testing*, German Institute for Standardization, Berlin.

Eurocode No. 2, Final Draft (2003), *Design of Concrete Structures – Part 1-1 : GENERAL Rules and Rules for Buildings*, Commission of the European Communities, Brussels.

LNEC Varoes de ac (2008), "A400 NR de ductilidade especial para armaduras de betao armado caracteristıcas, ensaios e marcac", AO, LNEC E455-2008.

UNE (2000), "Norma Espanola experimental barras corrugadas de acero soldable con caracteristıcas especiales de ductilidad para armaduras de horigon armado", UNE 36065 EX 2000, Madrid.

Corresponding author
Konstantinos Koulouris can be contacted at: kkoulouris@upnet.gr

For instructions on how to order reprints of this article, please visit our website:
www.emeraldgrouppublishing.com/licensing/reprints.htm
Or contact us for further details: **permissions@emeraldinsight.com**